

Supplementary Information

# Oxide nanoparticle exsolution in Lu-doped (Ba,Lu)CoO<sub>3</sub>

Daria Balcerzak<sup>1</sup>, Iga Szpunar<sup>1</sup>, Ragnar Strandbakke<sup>2</sup>, Sarmad W. Saeed<sup>2</sup>, Calliope Bazioti<sup>3</sup>, Aleksandra Mielewczyk-Gryń<sup>1</sup>, Piotr Winiarz<sup>4</sup>, Alfonso J. Carrillo<sup>5</sup>, María Balaguer<sup>5</sup>, Jose M. Serra<sup>5</sup>, Maria Gazda<sup>1</sup>, Sebastian Wachowski<sup>1</sup>

<sup>1</sup> Institute of Nanotechnology and Materials Engineering, Faculty of Applied Physics and Mathematics, and Advanced Materials Centre, Gdańsk University of Technology, Gdańsk, Poland

<sup>2</sup> Department of Chemistry, Centre for Materials Science and Nanotechnology, University of Oslo, 0371 Oslo, Norway

<sup>3</sup> Department of Physics, Centre for Materials Science and Nanotechnology, University of Oslo, 0371 Oslo, Norway

<sup>4</sup> Department of Hydrogen Energy, Faculty of Energy and Fuels, AGH University of Science and Technology, Kraków, Poland

<sup>5</sup> Instituto de Tecnología Química, Universitat Politècnica de València-Consejo Superior de Investigaciones Científicas, Avenida Los Naranjos s/n, 46022 Valencia, Spain

## 1. Determination of phase composition for specimen with various Lu-contents

XRD data of the synthesized materials with various content of Lu are presented in Figure S1. The attempted chemical compositions were Ba<sub>0.5</sub>La<sub>0.4</sub>Lu<sub>0.1</sub>CoO<sub>3</sub>, Ba<sub>0.5</sub>La<sub>0.475</sub>Lu<sub>0.025</sub>CoO<sub>3-δ</sub>, Ba<sub>0.5</sub>La<sub>0.485</sub>Lu<sub>0.015</sub>CoO<sub>3-δ</sub> and Ba<sub>0.5</sub>La<sub>0.495</sub>Lu<sub>0.005</sub>CoO<sub>3-δ</sub>. Secondary phase formation (red ticks) indicates that Lu doping always leads to decomposition and no Lu doping on A-site can be achieved.

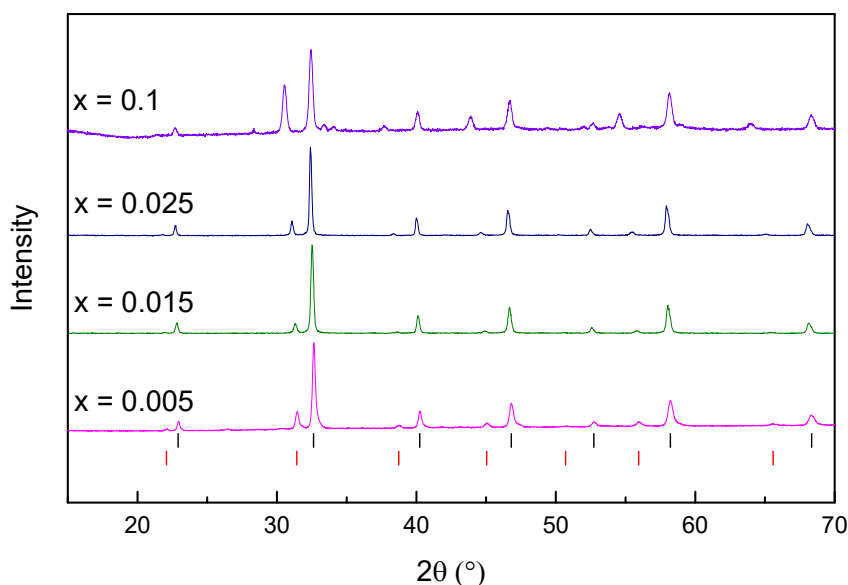


FIGURE S1 XRD data of as-synthesized Ba<sub>0.5</sub>La<sub>0.5-x</sub>Lu<sub>x</sub>CoO<sub>3</sub> (x = 0.005, 0.015, 0.025, 0.1) powders. Bragg positions of the main phase (BLCO-Lu) are indexed by black vertical ticks, for the secondary BCO-Lu phase – the red one was used.

The Rietveld refinement results are summarized for each composition in Table S1. The weight phase fraction ( $f$ ) data, determined in wt. % units, for each from the detected phase, is presented. It is seen that with decreasing amount of lutetium, the additional phase of BCO-Lu content is also diminishing. However, even for the smallest Lu content (0.5 mol. %), the secondary phase was detected, which points to high instability of the structure due to rare-earth metal doping. What is more, the third phase of BaLuCo<sub>4</sub>O<sub>7</sub> was not observed for a small amount of dopant. This was expected since for 10% doping the amount of BaLuCo<sub>4</sub>O<sub>7</sub> was close to the detection limit.

TABLE S1 Weight phase fractions (wt. %) of the as-synthesized samples of different Ba<sub>0.5</sub>La<sub>0.5-x</sub>Lu<sub>x</sub>CoO<sub>3</sub> composition (where  $x = 0.005, 0.015, 0.025, 0.1$ ) with Rietveld refinement coefficient results.

Lu content (mol. %)	10 (Reference)	2.5	1.5	0.5
BLCO-Lu wt. %	77	89	92	93
BCO-Lu wt. %	17	11	8	7
BaLuCo <sub>4</sub> O <sub>7</sub> wt. %	6	—	—	—
R <sub>w</sub> (%)	1.9	14.7	15.1	3.1
GOF	3.9	1.2	1.2	2.0

### 1.1. Structural analysis of the sample with 10% of Lu dopant

The unit cell parameters ( $a$ ,  $c$ ) and the weight fractions along with refinement agreement indices ( $R_w$ ,  $GOF$ ) of the BLCO-Lu, BCO-Lu; and BaLuCo<sub>4</sub>O<sub>7</sub> phases in the synthesized and annealed samples are summarized in Table S2. According to Rietveld refinement, the annealing does not lead to significant changes in unit cell parameters. After annealing at 1200 °C the amount of the main BLCO-Lu phase decrease with a simultaneous increase of that of BCO-Lu. In most cases, the BaLuCo<sub>4</sub>O<sub>7</sub> phase content remains constant and is around 5-6 wt. %. With lowering the temperature to 1000 °C and 800 °C, the trend is similar, and the content of the main BLCO-Lu and BCO-Lu phases is close to that annealed at 1200 °C. After annealing at 600 °C, the increase of the BCO-Lu and BaLuCo<sub>4</sub>O<sub>7</sub> phases content at the expense of BLCO-Lu drop (to 67 wt. % from 77 wt. %) is seen. This is the only sample, where the change of BaLuCo<sub>4</sub>O<sub>7</sub> phase content is not below the uncertainty limit of the method. At the lowest temperature, 400 °C, the content of the main phase is close to that of the as-prepared specimen.

TABLE S2 Unit cell parameters (Å), weight phase fractions (wt. %) and Rietveld refinement coefficient results (%) of the BLCO-Lu, BCO-Lu; and BaLuCo<sub>4</sub>O<sub>7</sub> phases in the synthesized and annealed samples obtained with the use of the Rietveld refinement.

Conditions	BLCO-Lu ( $Pm\bar{3}m$ )		BCO-Lu ( $Pm\bar{3}m$ )		BaLuCo <sub>4</sub> O <sub>7</sub> ( $P3_1c$ )			Refinement coefficients	
	a (Å)	wt.%	a (Å)	wt. %	a (Å)	c (Å)	f (wt. %)	R <sub>w</sub> (%)	GOF
1200°C, slowly cooled	3.87379	77	4.0895	17	6.25588	10.2339	6	1.9	3.9
1200 °C, quenched	3.87989	68	4.09278	27	6.27156	10.22957	5	15.9	2.3
1000 °C, quenched	3.87311	74	4.1039	20	6.26408	10.22349	6	12.9	2.1
800 °C, quenched	3.87982	74	4.08728	21	6.26539	10.22812	5	12.7	1.8

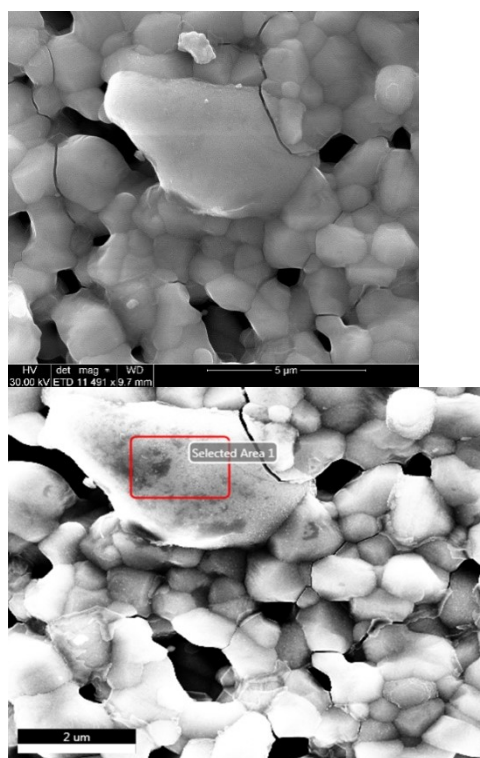
<b>600 °C, quenched</b>	3.87123	67	4.09457	25	6.25312	10.21907	8	18.6	1.7
<b>400 °C, quenched</b>	3.87318	76	4.08721	18	6.25038	10.22184	6	13.2	1.9

It should be noted that all of the annealed samples were quenched to room temperature, therefore the measured crystal structure should retain the characteristics and represent the properties of the materials at annealing temperatures.

## 2. Investigation of the sample annealed at 600 °C

### 2.1. Chemical composition

The sample annealed at 600 °C is the one in which the presence of the  $\text{BaLuCo}_4\text{O}_7$  phase was confirmed by EDX. The SEM images with the percentage content of detected elements are summarized in Figure S2. This shows agreement with the indications from Rietveld refinement that the  $\text{BaLuCo}_4\text{O}_7$  phase content increases after annealing at 600 °C.



Element	At. (%)
<b>O</b>	55
<b>Co</b>	32
<b>Ba</b>	8
<b>Lu</b>	5

FIGURE S2 SEM images in SE mode (left) in BSE mode (middle) with atomic content in table EDX measurement based on Area 1 from SEM image of the grain obtained at 600 °C.

### 2.2. Microstructural analysis

The microstructure and NP characteristics were investigated with SEM imaging with the use of two different modes. First, the BSE mode was applied to observe whether grain segregation was similar to that at other temperatures. The result shown in Figure S3 a) presents two different areas. On the right side of the SEM image, phase differentiation in adjacent grains can be observed. However, on the left side, the elongated crystals are covering the surface. The NPs were also detected at this temperature, exsolved between the crystals (see Figure S3 b).

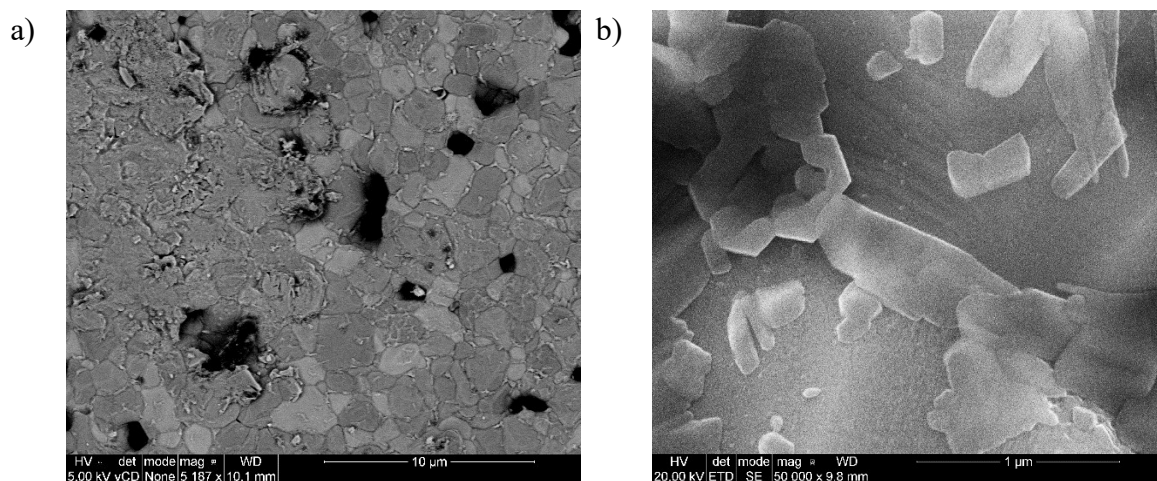
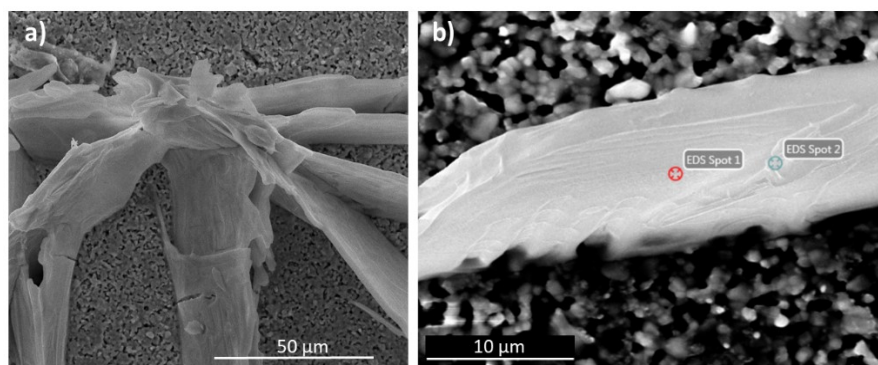


FIGURE S3 SEM image of the sample a) with the boundary between elongated crystals covered the surface (left side) and with a non-covered surface (right side) taken in BSE mode, and b) SEM image of NPs presence in SE mode in 10 times higher magnification.

### 3. Chemical composition investigation of the sample annealed at 1000 °C

The sample annealed at 1000 °C is unique in all studies. In contrast to other samples, this specimen image of the surface shows a porous microstructure with a uniform shade of grey. Moreover, the EDX result does not show clear changes in elemental composition between different grains. It is consistent with Rietveld refinement, where the phase fraction of the parent phase was the highest for this sample ( $f_{\text{BLCO-Lu}} = 74\%$ ). For this sample, additional studies revealed a large, plate-like grain, which is presented in Figure S4.



Element	At. (%)	
	Spot 1	Spot 2
O	55	53
C	27	27
Co	5	3
Ba	10	14
La	2	2
Lu	1	1

FIGURE S4 SEM images of a) a sample annealed at 1000 °C in magnification 1 thousand times in immersive mode and b) a plate crystal with summarized content of elements detected by EDX from marked spots 1 and 2.

It reaches about hundreds of micrometres and has grown from the substrate in the shape of plates. The imaging in BSE mode shows a slight difference in the contrast in the SEM image. The chemical composition was analysed by the means of EDX. The results were presented in Figure S4 b), and show a high content of barium and carbon. It indicates the presence of barium carbonate. Interestingly, the barium carbonate phase was not observed in the XRD results. However, the presence of large barium carbonate grains and porous microstructure indicates that the sample quenched from 1000 °C underwent partial decomposition. The decomposition happened most probably after quenching. This sample right after quenching was identical in colour to all other specimens. After a couple of hours, bright deposits became visible to the naked eye on the material surface. These deposits are probably the barium carbonate observed in SEM. It can be concluded, that at 1000 °C annealed sample is meta-stable, and possibly

differs in composition from others. This would explain the differences in XRD refinement results and observed microstructure.

#### 4. Microstructure investigation of the annealed sample

##### 4.1. 1200 °C

Investigation of the microstructure of the sample annealed at 1200 °C by SEM is presented in Figure S5. The nanoparticles exsolved on different grains, both in BLCO-Lu and BCO-Lu phases. The phase contrast between these grains is visible due to the BSE mode used during SEM imaging. The exsolved nanoparticles also show different contrast compared to the substrate.

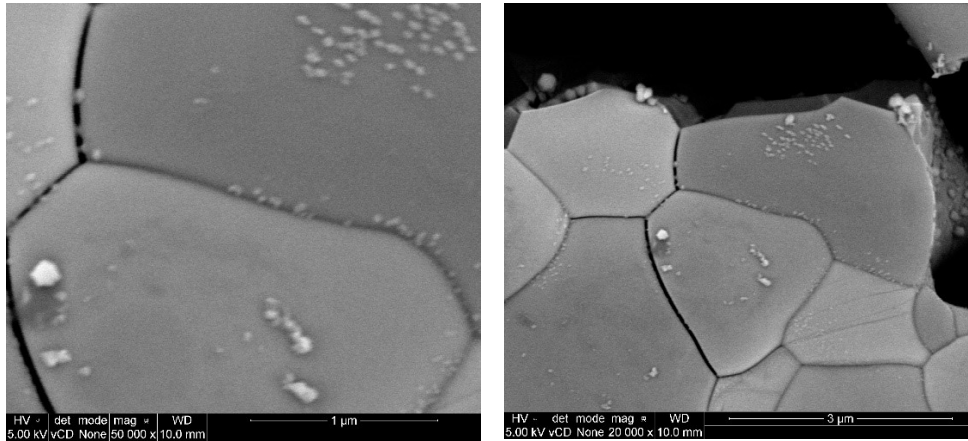


FIGURE S5 SEM images obtained in BSE mode of the sample annealed at 1200 °C in different magnifications.

##### 4.2. 800 °C

Observation with the use of SEM technique in BSE mode of the microstructure of sample annealed at 800 °C is presented in Figure S6. It shows the differentiation in adjacent grains and the tendency of exsolving the nanoparticles in the main BLCO-Lu phase. The image confirms also the phase contrast between nanoparticles and grains. Two types of different shapes of particles are visible; small and spherical NPs exsolved on BLCO-Lu grains and larger cuboidal NPs on the grain boundaries.

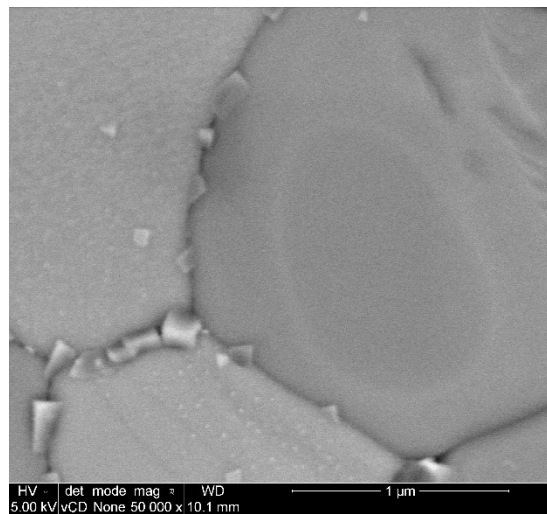


FIGURE S6 SEM image obtained in BSE mode of the sample annealed at 800 °C.

### 4.3. 400 °C

As in the case of higher temperatures, also at 400 °C, we observe phase differentiation of grains on the sample surface. The SEM image obtained in BSE mode is presented in Figure S7. It can be observed that nanoparticles exsolved on both phases, and the phase differentiation between the substrate and NPs is detectable in the BSE mode. No significant differences are noticed between the shape of NPs exsolved in two different phases.

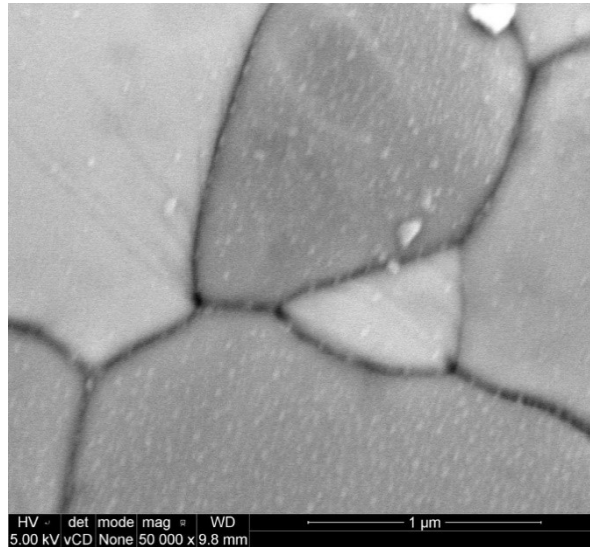


FIGURE S7 SEM image obtained in BSE mode of the sample annealed at 400 °C.